Article

Crystal Structures of *n*-BuLi Adducts with (*R*,*R*)-TMCDA and the Consequences for the Deprotonation of Benzene

Carsten Strohmann, and Viktoria H. Gessner

J. Am. Chem. Soc., **2008**, 130 (35), 11719-11725 • DOI: 10.1021/ja8017187 • Publication Date (Web): 08 August 2008

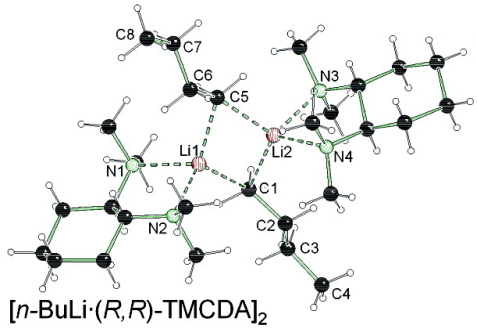

[*n*-BuLi·(*R*,*R*)-TMCDA]$_2$

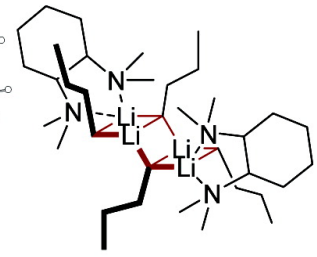

[(*n*-BuLi)$_2$·(*R*,*R*)-TMCDA]$_2$

More About This Article

Additional resources and features associated with this article are available within the HTML version:

- Supporting Information
- Access to high resolution figures
- Links to articles and content related to this article
- Copyright permission to reproduce figures and/or text from this article

View the Full Text HTML

J|A|C|S
ARTICLES

Published on Web 08/08/2008

Crystal Structures of *n*-BuLi Adducts with (*R*,*R*)-TMCDA and the Consequences for the Deprotonation of Benzene

Carsten Strohmann* and Viktoria H. Gessner

Institut für Anorganische Chemie, Universität Würzburg, Am Hubland, 97074 Würzburg, Germany

Received October 30, 2007; E-mail: mail@carsten-strohmann.de

Abstract: Combinations of organolithium compounds and diamine bases have become a powerful tool in synthetic chemistry. Because of the structure−reactivity relationship, the elucidation of reaction mechanisms of these reagents is strongly connected with the structural determination of intermediate species. In mixtures of the diamine TMCDA (*N*,*N*,*N*′,*N*′-tetramethylcyclohexane-1,2-diamine) and *n*-butyllithium, two different structures, the dimeric [*n*-BuLi·(*R*,*R*)-TMCDA]$_2$ and the aggregate [(*n*-BuLi)$_2$·(*R*,*R*)-TMCDA]$_2$, can be isolated, depending on the *n*-BuLi/TMCDA ratio. Thereby, [(*n*-BuLi)$_2$·(*R*,*R*)-TMCDA]$_2$ is a rare example of an organolithium compound with a ladder arrangement of the central four-membered Li−C−Li−C rings. Two isomers of the ladder structure are formed in the crystal by changing from the enantiomerically pure to racemic TMCDA. As *n*-BuLi/TMCDA mixtures are also able to deprotonate benzene, these structures give hint to possible mechanisms. Supported by theoretical studies, transition states based on the dimer, the ladder structure, and a hypothetical monomer are discussed.

Introduction

Deprotonation reactions with organolithium bases are among the most important reactions in synthetic chemistry. Their application ranges from simple deprotonations and directed ortholithiations to highly selective asymmetric deprotonations. Especially, otholithiations of functionalized aromates have gained central importance in organic chemistry, due to their high regioselectivities. Seminal work on this field was done by Wittig and Gilman in the 1930s.[1] The mechanistic pathway of these lithiations is often supposed to proceed via a precoordinated complex according to the complex-induced proximity effect (CIPE).[2,3] In this complex, the directing group (e.g., methoxy) brings the lithium base in proximity to the acidic hydrogen atom, resulting in high regio- or stereoselectivities. However, also different mechanisms are discussed, particularly the intrinsic acidifying effect by the functional group (Figure 1).[4] Alternative pathways to the CIPE model are necessary, especially for the clarification of the mechanisms of reactions involving CH-acidic compounds without functional groups, such as benzene. Hereby, activation by strong ligands, such as the diamine TMEDA (*N*,*N*,*N*′,*N*′-tetramethylethylenediamine), is generally required, and reaction mechanisms involving triple ions, open dimers, and small aggregates such as monomers and dimers with open reaction sites have been proposed.[5] Thus, the clarification of reactive intermediates is a central task for the understanding of the ongoing processes in these reactions.

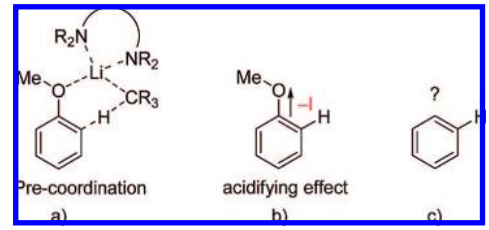

Figure 1. Deprotonation of anisole via (a) the CIPE mechanism and (b) the acidifying effect.

Most recently, we reported on the crystal structures of combinations of the diamine (1*R*,2*R*)-*N*,*N*,*N*′,*N*′-tetramethylcyclohexane-1,2-diamine [(*R*,*R*)-TMCDA] (**1**) with lithium alkyls and their ability to deprotonate benzene even with substoichio-

(1) (a) Wittig, G.; Pockels, U.; Droge, H. *Chem. Ber.* **1938**, *71*, 1903. (b) Gilman, H.; Bebb, R. L. *J. Am. Chem. Soc.* **1939**, *61*, 109.
(2) For the complex-induced proximity effect, see: (a) Whisler, M. C.; MacNeil, S.; Snieckus, V.; Beak, P. *Angew. Chem., Int. Ed.* **2004**, *43*, 2206. (b) Hartung, C. G.; Snieckus, V. In *Modern Arene Chemistry*; Astruc, D., Ed.; Wiley-VCH: Weinheim, Germany, 2002; pp 330−367. (c) Beak, P.; Meyers, A. I. *Acc. Chem. Res.* **1986**, *19*, 356.
(3) For *ortho*-metalations, see: (a) Slocum, D. W.; Dumbris, S.; Brown, S.; Jackson, G.; LaMastus, R.; Mullins, W.; Ray, J.; Shelton, P.; Walstrom, A.; Wilcox, J. M.; Holman, R. W. *Tetrahedron* **2003**, *59*, 8275. (b) Slocum, D. W.; Carroll, A.; Dietzel, P.; Eilermann, S.; Culver, J. P.; McClure, B.; Brown, S.; Holman, R. W. *Tetrahedron Lett.* **2006**, *47*, 865. (c) Slocum, D. W.; Dietzel, P. *Tetrahedron Lett.* **1999**, *40*, 1823. (d) Chadwick, S. T.; Ramirez, A.; Gupta, L.; Collum, D. B. *J. Am. Chem. Soc.* **2007**, *129*, 2259. (e) Rennels, R. A.; Maliakal, A. J.; Collum, D. B. *J. Am. Chem. Soc.* **1998**, *120*, 421. (f) Manolis, S. *J. Org. Chem.* **1997**, *62*, 3024.
(4) (a) Roberts, J. D.; Curtin, D. Y. *J. Am. Chem. Soc.* **1946**, *68*, 1658. (b) Fuhrer, W.; Gschwend, H. W. *J. Org. Chem.* **1979**, *44*, 1133. (c) Fitt, J. J.; Gschwend, H. W. *J. Org. Chem.* **1976**, *41*, 4029.
(5) (a) Adler, H. J.; Lochmann, L.; Dotcheva, D. T.; Tsvetanov, C. B. *Macromolecules* **1986**, *187*, 1253. (b) Gill, J. B. *Pure Appl. Chem.* **1987**, *59*, 1127. (c) Pauer, F.; Rocha, J.; Stalke, D. *J. Chem. Soc., Chem. Commun.* **1991**, 1477. (d) Eiermann, M.; Hafner, K. *J. Am. Chem. Soc.* **1992**, *114*, 135. (e) Williard, P. G.; Liu, Q.-Y. *J. Am. Chem. Soc.* **1993**, *115*, 3380. (f) Romesberg, F. E.; Collum, D. B. *J. Am. Chem. Soc.* **1994**, *116*, 9187. (g) Gornitzka, H.; Stalke, D. *Angew. Chem., Int. Ed. Engl.* **1994**, *33*, 693. (h) Reich, H. J.; Sikorski, W. H.; Gudmundsson, B. Oe.; Dykstra, R. R. *J. Am. Chem. Soc.* **1998**, *120*, 4035. (i) Chadwick, S. T.; Rennels, R. A.; Rutherford, J. L.; Collum, D. B. *J. Am. Chem. Soc.* **2000**, *122*, 8640. (j) Collum, D. B.; McNeil, A. J.; Ramirez, A. *Angew. Chem., Int. Ed.* **2007**, *46*, 3002.

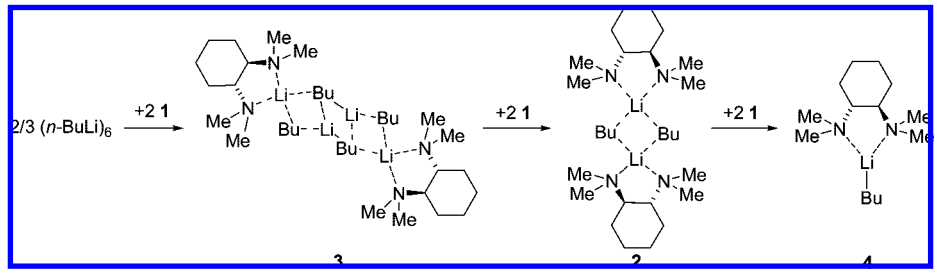

Figure 2. *n*-Butyllithium adducts with (*R*,*R*)-TMCDA.

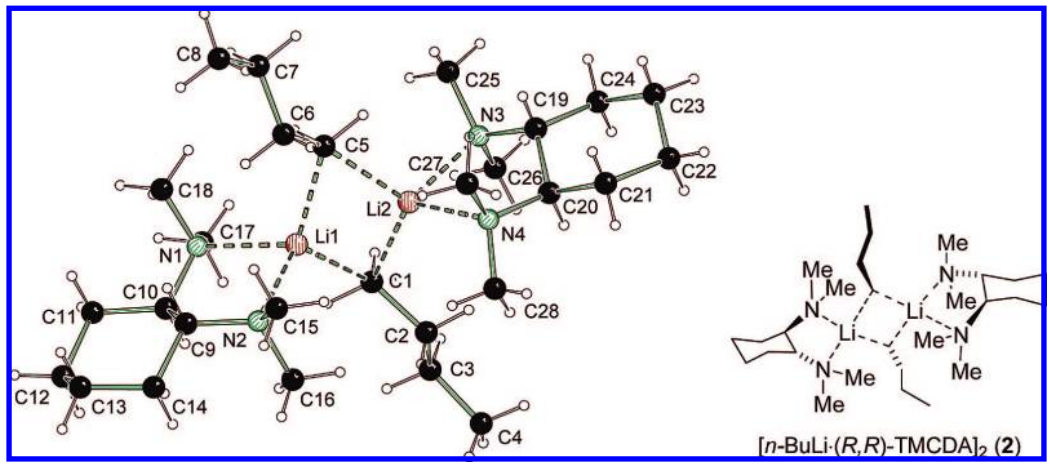

Figure 3. Molecular structure and drawing of [*n*-BuLi·(*R*,*R*)-TMCDA]$_2$ (**2**) in the crystal. Selected bond lengths (Å) and angles (deg): Molecule 1, C1−Li1, 2.279(6); C1−Li2, 2.233(7); C5−Li1, 2.214(6); C5−Li2, 2.261(6); Li1−N1, 2.192(6); Li1−N2, 2.179(7); Li2−N3, 2.189(6); Li2−N4, 2.134(6); Li1−C5−Li2 66.80(12), Li1−C1−Li2 66.2(2), C5−Li1−C1 110.1(3), C1−Li2−C5 110.1(3); Molecule 2, C(33)−Li(3) 2.199(7), C(33)−Li(4) 2.219(7), C(29A)−-Li(4) 2.32(2), C(29B)−Li(3) 2.268(17), Li(3)−N(5) 2.151(7), Li(3)−N(6) 2.160(7), Li(4)−N(8) 2.138(7), Li(4)−N(7) 2.221(7), Li(3)−C(33)−Li(4) 67.8(2), C(33)−Li(3)−C(29B) 111.5(4), C(33)−Li(4)−C(29A) 111.2(6), Li(3)−C(29A)−Li(4) 65.5(4).

metric amounts of the amine.[6] Based on such structures of adducts between lithium bases and diamine ligands, the question arises: How does the mechanism of deprotonation reactions with such adducts proceed?

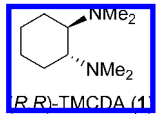

We report herein the structural elucidations with the most important lithium alkyl, *n*-butyllithium, and (*R*,*R*)-TMCDA (**1**) as Lewis base. Two different types of structures, depending on the concentration of the lithium compound, are presented, the dimeric [*n*-BuLi·(*R*,*R*)-TMCDA]$_2$ (**2**) and the aggregate [(*n*-BuLi)$_2$·(*R*,*R*)-TMCDA]$_2$ (**3**) (Figure 2), the latter of which is the first homoaggregate of an alkyllithium base with a ladder arrangement. Both structures prompted us to take a closer glance at the possible mechanistic pathways of the lithiation of benzene by examining various adducts of (*R*,*R*)-TMCDA (**1**) and *n*-BuLi, which were modeled after the structures discovered in the crystal.

Results and Discussion

Crystal Structures of *n*-BuLi. The dimeric adduct [*n*-BuLi·(*R*,*R*)-TMCDA]$_2$ (**2**) crystallizes from *n*-pentane/hexane at −78 °C in the monoclinic crystal system, space group *C*2 (two molecules were detected in the asymmetric unit, one of which is shown in Figure 3).[7] The central structural motif of this aggregate is a central four-membered Li−C−Li−C ring, as is typical for dimeric alkyllithium compounds.[8] The Li−C−Li−C ring shows a slight deformation from planarity toward an envelope conformation (sum of ring angles 353.2°). The butyl groups are arranged on different sides of the Li_2C_2 ring, one above and the other one below the ring. The Li−C distances range from 2.214(6) to 2.279(6) Å, the Li−N distances from 2.134(6) to 2.192(6) Å, and are thus comparable with the three other known dimeric *n*-BuLi adducts.[9] This dimeric *n*-butyllithium structure has already been predicted by NMR studies conducted by D. B. Collum and co-workers.[10]

Using 2 equiv of *n*-butyllithium results in a change of the degree of aggregation with the formation of [(*n*-BuLi)$_2$·(*R*,*R*)-TMCDA]$_2$ (**3a**) (Figure 4). The aggregate crystallizes from *n*-pentane/hexane at −50 °C in the monoclinic crystal system,

(6) (a) Strohmann, C.; Gessner, V. H. *J. Am. Chem. Soc.* **2007**, *129*, 5982. (b) Strohmann, C.; Gessner, V. H. *Angew. Chem., Int. Ed.* **2007**, *46*, 8281.

(7) X-ray crystallography data for **1**, **2**, and **3** have been deposited with the Cambridge Crystallographic Data Center as supplementary publication nos. CCDC 658072 (**2**), CCDC 658071 (**3a**), and CCDC 658070 (**3b**).

(8) Stey, T.; Stalke, D. In *The Chemistry of Organolithium Compounds*; Rappoport, Z., Marek, I., Eds.; Wiley: Chichester, 2004; Chapter 2.

(9) (a) Nichols, M. A.; Williard, P. G. *J. Am. Chem. Soc.* **1993**, *115*, 1568. (b) Barnett, N. D. R.; Mulvey, R. E. *J. Am. Chem. Soc.* **1993**, *115*, 1573. (c) Strohmann, C.; Strohfeldt, K.; Schildbach, D. *J. Am. Chem. Soc.* **2003**, *125*, 13672. (d) Strohmann, C.; Gessner, V. H. *Angew. Chem., Int. Ed.* **2007**, *46*, 4566.

(10) (a) Hoffmann, D.; Collum, D. B. *J. Am. Chem. Soc.* **1998**, *120*, 5810. (b) Rutherford, J. L.; Hoffmann, D.; Collum, D. B. *J. Am. Chem. Soc.* **2002**, *124*, 264.

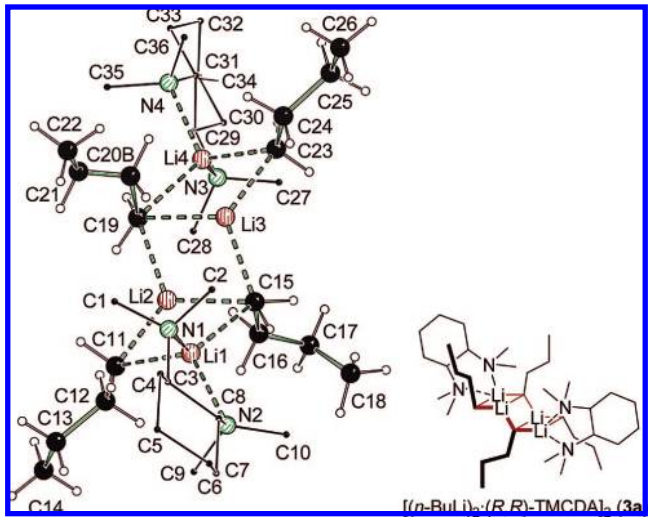

Figure 4. Molecular structure and drawing of $[(n\text{-BuLi})_2\cdot(R,R)\text{-TMCDA}]_2$ (**3a**). Selected bond lengths (Å) and angles (deg) (hydrogen atoms of the cyclohexane ring are omitted for clarity): C11−Li1, 2.353(5); C11−Li2, 2.234(6); C11−Li3, 2.158(6); C15−Li1, 2.183(5); C15−Li2, 2.134(6); C19−Li3, 2.122(5); C19−Li4, 2.199(5); C23−Li2, 2.193(7); C23−Li3, 2.181(6); C23−Li4, 2.194(6); Li1−N1, 2.105(4); Li1−N2, 2.096(5); Li4−N3, 2.074(5); Li4−N4, 2.145(5): Li(2)−C(11)−Li(1), 63.68(17); Li(2)−C(15)−Li(1),68.28(18);C(15)−Li(2)−C(11),115.3(2);C(15)−Li(1)−C(11), 108.9(2); Li(3)−C(19)−Li(4), 67.67(219); Li(3)−C(23)−Li(4), 63.53(17); C(19)−Li(3)−C(23), 116.0(2); C(19)−Li(4)−C(23), 106.4(2).

space group $P2_1$. The central motif of this structure is formed by three four-membered Li−C−Li−C rings with a ladder arrangement. The rings show deformations from planarity (sum of ring angles 356.2°, 359.6°, and 353.6°) and are not arranged rectangularly to each other. The two external lithium centers are coordinated by the two (*R*,*R*)-TMCDA molecules, having thus four contacts each: two to the nitrogen centers and two to the carbanion centers. The interior lithium centers possess only three contacts to the carbanion centers. The Li−C distances range from 2.125(6) to 2.359(6) Å and the Li−N from 2.073(6) to 2.148(5) Å, and are thus comparable with monomeric and dimeric organolithium compounds and also with the hexameric parent structure $(n\text{-BuLi})_6$.[8,9,11,12] **3a** is the first homoaggregate of *n*-butyllithium with a ladder arrangement of the central four-membered Li−C−Li−C rings.[13] A comparable structure has only been detected with phenyllithium as lithium base.[12]

Interestingly, a further isomer of the ladder structure **3** can be isolated from a mixture of the racemic amine with 2 equiv of *n*-butyllithium (Figure 5). In this isomer, only the like-products, $[(n\text{-BuLi})_2\cdot(R,R)\text{-TMCDA}]_2$ and $[(n\text{-BuLi})_2\cdot(S,S)\text{-TMCDA}]_2$, crystallize in the triclinic crystal system, space group

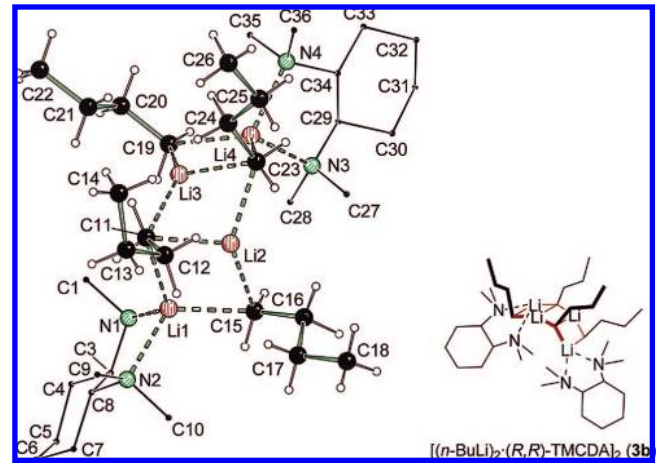

Figure 5. Molecular structure and drawing of isomer $[(n\text{-BuLi})_2\cdot(R,R)\text{-TMCDA}]_2$ (**3b**). Selected bond lengths (Å) and angles (deg) (hydrogen atoms of the cyclohexane ring are omitted for clarity): C11−Li1, 2.314(6); C11−Li2, 2.226(6); C11−Li3, 2.212(6); C15−Li1, 2.216(6); C15−Li2, 2.112(7); C19−Li3, 2.131(6); C19−Li4, 2.219(6); C23−Li2, 2.210(7); C23−Li3, 2.222(6); C23−Li4, 2.327(6); Li1−N1, 2.086(6); Li1−N2, 2.191(5); Li4−N3, 2.106(5); Li4−N4, 2.151(5); Li(2)−C(11)−Li(1), 64.9(2); Li(2)−C(15)−Li(1), 68.5(2); C(15)−Li(1)−C(11), 109.2(2); C(15)−Li(2)−C(11),116.7(3);Li(3)−C(11)−Li(2),63.2(2);Li(2)−C(23)−Li(3), 63.3(2); C(23)−Li(2)−C(11), 101.6(3); C(11)−Li(3)−C(23), 101.7(2); Li(3)−C(19)−Li(4),67.8(2);Li(3)−C(23)−Li(4),64.5(2);C(19)−Li(3)−C(23), 117.3(3); C(19)−Li(4)−C(23), 109.7(2).

$P\bar{1}$ to give compound **3b** (two molecules were detected in the asymmetric unit; only the (*R*,*R*)-TMCDA adduct is shown in Figure 5). Numerous measurements of compound **3b** always showed crystals of this space group. The crystallization of solely the (*R*,*R*)-TMCDA or (*S*,*S*)-TMCDA adduct such as in compound **3a** was not detected. As in isomer **3a**, the Li−C−Li−C rings show deformation from planarity (sum of ring angles 359.3°, 229.7°, and 359.3°) and no rectangular arrangement. The Li−C and Li−N distances vary in a range typical for monomers and dimers and also for $(n\text{-BuLi})_6$.[8,9,11−13]

Both isomers of **3** differ in the arrangement of the central ladder unit. Whereas in **3b** all *n*-butyl groups are orientated on the same side of the Li−C−Li−C four-membered rings, the *n*-butyl units of **3a** are alternating below and above the Li−C−Li−C rings. This results in a "real" ladder arrangement of **3a**, whereas isomer **3b** possesses an arch-like arrangement (Figures 4 and 5). Taken together, both isomers of **3** describe a stepwise transition from the hexameric parent structure $(n\text{-BuLi})_6$ to the dimeric compound **2**. This can be demonstrated by means of the Li−C contacts. Whereas the carbon atoms in the hexameric compound with its characteristic Li_3C units possess three contacts each, the carbon atoms in the dimeric $[n\text{-BuLi}\cdot(R,R)\text{-TMCDA}]_2$ (**2**) have two contacts. Structure **3** contains both types of carbon atoms and thus represents the transition from $(n\text{-BuLi})_6$ to the dimer.

Computational Studies: Crystal Structures. The formation of both isomers of $[(n\text{-BuLi})_2\cdot(R,R)\text{-TMCDA}]_2$ (**3**) can be understood by computational studies at the B3LYP/6-31+G(d) level showing an energetic difference of only 7 kJ/mol between the isomers (Figure 6).[14] Therefore, the observation of **3b** with racemic TMCDA and the absence of the crystallization of solely the (*R*,*R*)-TMCDA or (*S*,*S*)-TMCDA adduct such as in compound **3a** can be attributed to packing effects. Also, the formation of the dimeric compound $[n\text{-BuLi}\cdot(R,R)\text{-TMCDA}]_2$ (**2**) and the ladder structure $[(n\text{-BuLi})_2\cdot(R,R)\text{-TMCDA}]_2$ (**3**) can be understood by the energetic preference of **2** by 46 kJ/mol

(11) (a) Strohmann, C.; Seibel, T.; Strohfeldt, K. *Angew. Chem., Int. Ed.* **2003**, *42*, 4531. (b) Strohmann, C.; Dilsky, S.; Strohfeldt, K. *Organometallics* **2006**, *25*, 41. (c) Williard, P. G.; Sun, C. *J. Am. Chem. Soc.* **1997**, *119*, 11693.
(12) Kottke, T.; Stalke, D. *Angew. Chem., Int. Ed. Engl.* **1993**, *32*, 580.
(13) (a) Wijkens, P.; Jastrzebski, J. T. B. H.; Veldman, N.; Spek, A. L.; van Koten, G. *Chem. Commun.* **1997**, 2143. (b) Dinnebier, R. E.; Behrens, U.; Olbrich, F. *J. Am. Chem. Soc.* **1998**, *120*, 1430. (c) Donkervoort, J. G.; Vicario, J. L.; Rijnberg, E.; Jastrzebski, J. T. B. H.; Kooijman, H.; Spek, A. L.; van Koten, G. *J. Organomet. Chem.* **1998**, *463*, 463. (d) Strohmann, C.; Abele, B. C. *Organometallics* **2000**, *19*, 4173. (e) Strohmann, C.; Strohfeldt, K.; Schildbach, D.; McGrath, J.; O'Brien, P. *Organometallics* **2004**, *23*, 5389. (f) Vestergren, M.; Eriksson, J.; Hilmersson, G.; Håkansson, M. *J. Organomet. Chem.* **2003**, *682*, 172.
(14) Frisch, M. J.; et al. *Gaussian 03*, revision B.04; Gaussian, Inc.: Pittsburgh, PA, 2004.

over 1/3 (n-BuLi)$_6$ plus 2 (*R*,*R*)-TMCDA and of **3** by 46 and 39 kJ/mol over 2/3 (n-BuLi)$_6$ plus 2 (*R*,*R*)-TMCDA. Consequently, the formation of **2** and **3** can be controlled by the amount of the lithiumalkyl, as seen in experiment.

Computational Studies: Deprotonation of Benzene. Preliminary investigations by our group on the reactivity of analogous organolithium compounds indicated a high reactivity in deprotonation reactions like the direct lithiation of noncoordinating benzene.[6] As mixtures of n-BuLi and (*R*,*R*)-TMCDA showed a similar behavior in the experiment, the influence of the presented compounds **2** and **3** in the deprotonation of benzene should be investigated. DFT calculations were performed to gain a more detailed insight into the possible mechanisms of this deprotonation. The molecular structures of [n-BuLi·(*R*,*R*)-TMCDA]$_2$ (**2**) and [(n-BuLi)$_2$·(*R*,*R*)-TMCDA]$_2$ (**3**) were used as a starting point.[14] Structure optimization was performed at the B3LYP/6-31+G(d) level for all educts and transition states, and frequency analyses at the B3LYP/6-31G level to establish the nature of all stationary points.[15] All transition states showed only one imaginary frequency corresponding to the deprotonation. Reaction pathways via a monomer- and dimer-based transition state as well as via a transition state based on one-half of the ladder structure were investigated.

Transition States with *n*-Butyllithium. Two possible reaction pathways exist for the dimeric [n-BuLi·(*R*,*R*)-TMCDA]$_2$ and benzene: In the first case, the dimer **2** breaks into two n-BuLi·(*R*,*R*)-TMCDA (**4**) monomers (eq 1). These monomers are coordinated by benzene, which are then deprotonated via [n-BuLi·(*R*,*R*)-TMCDA·C$_6$H$_6$]‡ (**5**) (eq 2). In the second case, deprotonation occurs via the approach of benzene to the dimer (eq 3). Both transition states are depicted in Figure 7.

$$1/2[n\text{-BuLi}\cdot(R,R)\text{-TMCDA}]_2 \rightleftharpoons \underset{\mathbf{4}}{n\text{-BuLi}\cdot(R,R)\text{-TMCDA}} \quad (1)$$

$$n\text{-BuLi}\cdot(R,R)\text{-TMCDA} + C_6H_6 \xrightarrow{\Delta H^‡} \underset{\text{dimer-based TS (6)}}{\{[n\text{-BuLi}\cdot(R,R)\text{-TMCDA}]_2\cdot C_6H_6\}^‡} \quad (2)$$

$$[n\text{-BuLi}\cdot(R,R)\text{-TMCDA}]_2 + C_6H_6 \xrightarrow{\Delta H^‡} \underset{\text{dimer-based TS (6)}}{\{[n\text{-BuLi}\cdot(R,R)\text{-TMCDA}]_2\cdot C_6H_6\}^‡} \quad (3)$$

The mechanism via the dimer-based species {[n-BuLi·(*R*,*R*)-TMCDA]$_2$·C$_6$H$_6$}‡ (**6**) shows a barrier of 118 kJ/mol and the monomer-based transition state **5** a barrier of only 71 kJ/mol. However, the formation of monomeric n-BuLi·(*R*,*R*)-TMCDA out of dimer **2** (eq 1) requires 27 kJ/mol with an barrier that may even be higher. Considering entropy effects, the formation of the monomer becomes energetically more favored. However, for such polar compounds entropy is crucially influenced by solvent effects. Additionally, calculated Gibbs free energies in such large systems seem to be less reliable due to very low frequencies, where the harmonic oscillator model produces significant deviations.[16] Thus, enthalpy values are discussed.

Both the dimer- and the monomer-based mechanisms possess sufficiently low reaction barriers for the deprotonation. Thereby, the dimer-based pathway is in accordance with rate studies of the deprotonation of benzene by n-BuLi/TMEDA conducted by D. B. Collum.[5a] However, the existence of solely the dimer-based mechanism of the deprotonation of benzene with (*R*,*R*)-TMCDA can only be assumed when no equilibrium is reached between the monomer **4** and the dimer **2** (eq 1). This is the case, when the barrier of the conversion of both species into each other is high, so that deprotonation via the dimer occurs faster than the formation of the monomer. Considering n-BuLi and (*R*,*R*)-TMCDA, the monomer **4** is disfavored by only 27 kJ/mol over the dimer **2**, so that both mechanisms should be possible.

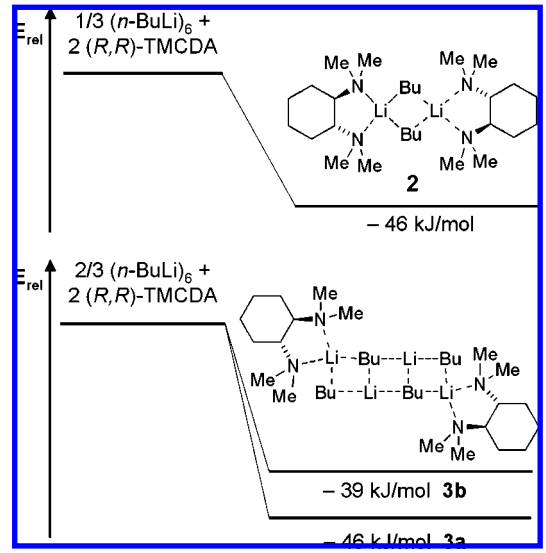

Figure 6. Formation of dimer **2** and both isomers of **3** out of hexameric (n-BuLi)$_6$ [B3LYP/6-31+G(d)].

Based on the ladder structure **3**, a mechanism via one-half of the ladder was calculated (Figure 8). Thereby, [(n-BuLi)$_2$·(*R*,*R*)-TMCDA]$_2$ (**3**) first breaks into two molecules of one-half of the ladder **7** (eq 4), which are then coordinated by benzene. Deprotonation occurs afterward via {[(n-BuLi)$_2$·(*R*,*R*)-TMCDA]·C$_6$H$_6$}‡ (**8**) showing a barrier of 90 kJ/mol (Figure 8). However, analogous to the monomer-based mechanism, the formation of one-half of the ladder requires 27 kJ/mol with a barrier, which is even higher. Although the barrier of the deprotonation itself is relatively low, the formation of one-half of the ladder is highly unlikely due to the almost naked lithium atom in the molecule. Instead of the coordination and deprotonation of benzene, the formation of the dimer **2** is energetically preferred by 51 kJ/mol (eq 6). However, using only catalytic amounts of the diamine such a mechanism via the ladder structure is imaginable.[3a−c]

$$1/2[(n\text{-BuLi})_2\cdot(R,R)\text{-TMCDA}]_2 \rightleftharpoons \underset{\mathbf{7}}{[(n\text{-BuLi})_2\cdot(R,R)\text{-TMCDA}]} \quad (4)$$

$$[(n\text{-BuLi})_2\cdot(R,R)\text{-TMCDA}] + C_6H_6 \xrightarrow{\Delta H^‡} \underset{\mathbf{8}}{\{[(n\text{-BuLi})_2\cdot(R,R)\text{-TMCDA}]\cdot C_6H_6\}^‡} \quad (5)$$

$$[(n\text{-BuLi})_2\cdot(R,R)\text{-TMCDA}] + (R,R)\text{-TMCDA} \rightleftharpoons \underset{\mathbf{2}}{[n\text{-BuLi}\cdot(R,R)\text{-TMCDA}]_2} \quad (6)$$

An alternative pathway for the deprotonation process is imaginable, in which the benzene molecule takes part in the deaggregation process. Hereby, the cleavage of the dimer to the monomer occurs via the approximation of benzene to the dimer, which breaks into two n-BuLi·(*R*,*R*)-TMCDA (**4**) monomers, one of which is coordinated by benzene (eq 7). The deprotonation occurs then again via [n-BuLi·(*R*,*R*)-

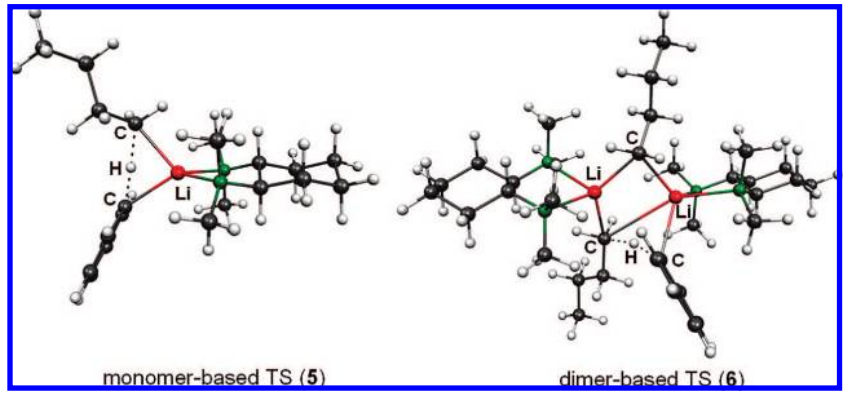

Figure 7. Calculated monomer-based (left) and dimer-based (right) transition structures.

TMCDA·C_6H_6]‡ (**5**) (eq 8). The total energy, required for this process, amounts to 124 kJ/mol, caused mainly by the loss of energy for breaking the dimer into the two monomeric species. The dimer-based pathway according to eq 3 showed a barrier of 128 kJ/mol. Consequently, this deaggregation−deprotonation process also indicates possible mechanisms involving monomeric and dimeric structures, analogous to the pathway via the pre-equilibrium between dimer and monomer (eq 1).

$$[n\text{-BuLi}\cdot(R,\underset{2}{R})\text{-TMCDA}]_2 + C_6H_6 \rightleftharpoons n\text{-BuLi}\cdot(R,\underset{4}{R})\text{-TMCDA} + \{[n\text{-BuLi}\cdot(R,R)\text{-TMCDA}]_2\cdot C_6H_6\} \quad (7)$$

$$n\text{-BuLi}\cdot(R,\underset{4}{R})\text{-TMCDA} + \{[n\text{-BuLi}\cdot(R,R)\text{-TMCDA}]_2\cdot C_6H_6\} \xrightarrow{\Delta H^{\ddagger}} n\text{-BuLi}\cdot(R,\underset{4}{R})\text{-TMCDA} + \{[n\text{-BuLi}\cdot(R,R)\text{-TMCDA}]_2\cdot C_6H_6\}^{\ddagger}_{\text{monomer-based TS (5)}} \quad (8)$$

For the ladder structure **3**, an analogous mechanism involving the approximation of benzene can be considered. Hereby, the ladder structure breaks into one-half of the ladder and one-half of the ladder coordinated by benzene (eq 9). Deprotonation occurs then again via one-half of the ladder structure {[*n*-BuLi]$_2$·(*R*,*R*)-TMCDA·C_6H_6}‡ (**8**), with a total barrier of 144 kJ/mol (eq 10). This barrier is also mainly caused by the breaking of the ladder structure and is too high to be overcome at room temperature.

$$[(n\text{-BuLi})_2\cdot(\underset{3}{R},R)\text{-TMCDA}]_2 + C_6H_6 \rightleftharpoons [(n\text{-BuLi})_2\cdot(\underset{7}{R},R)\text{-TMCDA}] + \{[(n\text{-BuLi})_2\cdot(R,R)\text{-TMCDA}]\cdot C_6H_6\} \quad (9)$$

$$[(n\text{-BuLi})_2\cdot(\underset{7}{R},R)\text{-TMCDA}] + \{[(n\text{-BuLi})_2\cdot(R,R)\text{-TMCDA}]\cdot C_6H_6\} \xrightarrow{\Delta H^{\ddagger}} [(n\text{-BuLi})_2\cdot(\underset{7}{R},R)\text{-TMCDA}] + \{[(n\text{-BuLi})_2\cdot(R,R)\text{-TMCDA}]\cdot C_6H_6\}^{\ddagger}_{\mathbf{8}} \quad (10)$$

Differences with Methyllithium as Model System. Analogous calculations have also been performed with methyllithium as lithium base. In literature, MeLi is often used as a model system for other organolithium compounds. However, methyllithium possesses a very strong tendency to build tetrameric structures, as was also found in experiment.[17] Because of that, the breaking to smaller adducts as dimers or monomers requires much energy. Thus, reaction pathways including the deaggregation to monomeric species are almost impossible because of the high loss of energy by breaking tetrameric $(MeLi)_4$ into monomers. Furthermore, reaction barriers with methyllithium as deprotonation reagent generally appear to be energetically higher than in comparison to butyllithium, especially with highly polar transition states. This increased barrier is probably due to a decreased charge distribution of methyllithium. Hence, in reactions involving deaggregation processes methyllithium is not an adequate model system.

The transition states of the deprotonation of benzene with methyllithium as lithium base are depicted in Figure 9. Thereby, the dimer-based transition state showed a barrier of 121 kJ/mol and the monomer-based mechanism a barrier of 73 kJ/mol. However, the cleavage of dimeric [MeLi·(*R*,*R*)-TMCDA]$_2$ to the monomer requires 39 kJ/mol, so that the existence of an equilibrium between monomer and dimer is less likely in comparison to butyllithium. The same is true for the mechanism via one-half of the ladder structure showing a barrier of 86 kJ/mol and a loss of 40 kJ/mol for the cleavage of the ladder structure.

Experimental Section

General Methods and Materials. All experiments were carried out under a dry, oxygen-free argon atmosphere using standard Schlenk techniques. Involved solvents were dried over sodium and distilled prior to use. (*R*,*R*)-TMCDA was synthesized by methylation of the enantiomeric pure tartaric salt, which was gained by racemic resolution as described in the literature.[18] *rac*-TMCDA was synthesized by methylation of the *trans*-amine (purchased from Aldrich Chemicals). The enantiomeric purity of (*R*,*R*)-TMCDA was determined by NMR spectroscopy (as described in the Supporting Information).

[*n*-BuLi·(*R*,*R*)-TMCDA]$_2$ (2). 170 mg (1.00 mmol) of (*R*,*R*)-TMCDA (**1**) was dissolved in 5 mL *of* *n*-pentane and cooled to −60 °C. At this temperature, 0.62 mL (0.99 mmol) of *n*-BuLi (1.6 M in hexane) was carefully added. Cooling to −78 °C gave [*n*-BuLi·(*R*,*R*)-TMCDA]$_2$ (**2**) as colorless needles after 4 h.

[(*n*-BuLi)$_2$·(*R*,*R*)-TMCDA]$_2$ (3a). 110 mg (0.65 mmol) of (*R*,*R*)-TMCDA (**1**) was dissolved in 5 mL of *n*-pentane and cooled to −78 °C. At this temperature, 0.81 mL (1.30 mmol) of *n*-BuLi (1.6 M in hexane) was carefully added. Warming up to −50 °C gave [(*n*-BuLi)$_2$·(*R*,*R*)-TMCDA]$_2$ (**3a**) as colorless needles.

[(*n*-BuLi)$_2$·*rac*-TMCDA]$_2$ (3b). 110 mg (0.65 mmol) of *rac*-TMCDA (*rac*-**1**) was dissolved in 5 mL of *n*-pentane and cooled to −78 °C. At this temperature, 0.81 mL (1.30 mmol) of *n*-BuLi (1.6 M hexane) was carefully added, and storage at −78 °C gave colorless needles of **3b** after 1 day.

Deprotonation of Benzene by *n*-BuLi·(*R*,*R*)-TMCDA. 170 mg (1.00 mmol) of (*R*,*R*)-TMCDA (**1**) was dissolved in 0.5 mL of benzene, and under cooling *n*-BuLi (1.6 M in hexane) was carefully added. The reaction mixture was slowly warmed to

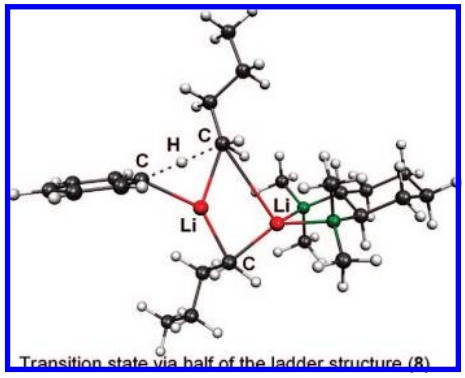

Figure 8. Calculated transition states of one-half of the ladder structure.

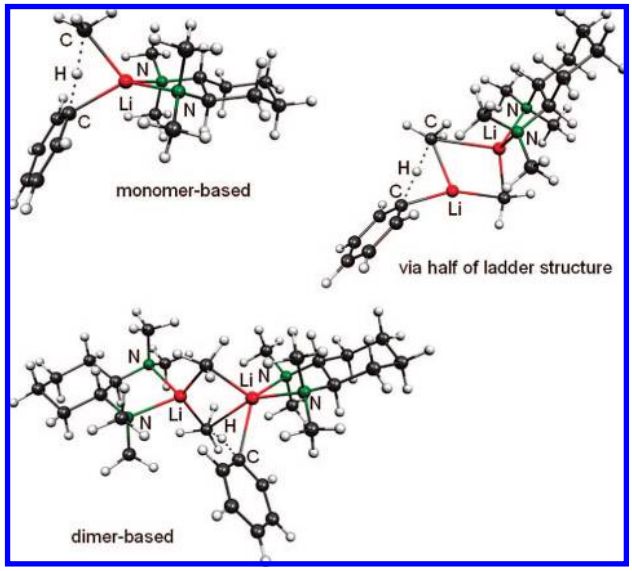

Figure 9. Calculated transition states with methyllithium as lithium base.

room temperature and afterward stirred for 2 h. After trapping with diphenylmethylchlorsilane, the reaction mixture was analyzed by NMR spectroscopy. The product mixtures obtained are shown in Table 1.

Table 1

n-BuLi (equiv)	Ph_3SiMe:$Ph_2MeSi(n\text{-}Bu)$
1	93:7
2	50:50

X-ray Structure Determination, General. [*n*-BuLi·(*R*,*R*)-TMCDA]$_2$ (**2**): Stoe IPDS diffractometer; data collection, Expose in IPDS (Stoe and Cie, 1999), cell determination and refinement, Cell in IPDS (Stoe and Cie, 1999); integration, Integrate in IPDS (Stoe and Cie, 1999); numerical absorption correction, Faceit in IPDS (Stoe and Cie, 1999). Compounds **3a** and **3b**: Bruker APEX-CCD (D8 three-circle goniometer) (Bruker AXS); data collection, cell determination and refinement, Smart version 5.622 (Bruker AXS, 2001); integration, SaintPlus version 6.02 (Bruker AXS, 1999); empirical absorption correction, Sadabs version 2.01 (Bruker AXS, 1999).

X-ray Structure Determination of 2. (colorless needles from *n*-pentane/hexane, 0.40 × 0.20 × 0.20 mm^3): $C_{28}H_{62}Li_2N_4$, M = 468.7, monoclinic, space group $C2$ (No. 5), a = 26.214(5), b = 8.3820(17), c = 29.429(6), V = 6466 (2) Å^3, Z = 8, D_c = 0.963 Mg m^{-3}, μ = 0.055 mm^{-1}. 23 498 reflections measured with 2θ in the range 2.55−25.00°, 10 906 unique reflections; 5521 with $I > 2\sigma(I)$; refinement by full-matrix least-squares methods (based on F_o^2, SHELXL-97); anisotropic thermal parameters for all non-H atoms in the final cycles; the H atoms were refined on a riding model in their ideal geometric positions, except for H(1A), H(1B), H(5A), H(5B), H(33A), and H(33B), which were refined independently; R1 = 0.0523 [$I > 2\sigma(I)$], wR2(F_o^2) = 0.0897 (all data), absolute structure (Flack) parameter 0(2). The refinement of the correct stereoisomer is unambiguous due to the fixed absolute configuration at C(9), C(10), C(19), and C(20) of the (*R*,*R*)-TMCDA (Flack parameter not significant).

X-ray Structure Determination of 3a. (colorless needles from *n*-pentane/hexane, 0.50 × 0.30 × 0.30 mm^3): $C_{36}H_{80}Li_4N_4$, M = 596.8, monoclinic, space group $P2_1$ (No. 4), a = 8.765(3), b = 25.083(8), c = 9466(3) Å, V = 2076.7(11) Å^3, Z = 2, D_c = 0.954 Mg m^{-3}, μ = 0.053 mm^{-1}. 29 729 reflections measured with 2θ in the range 1.62−25.00°, 7321 unique reflections; 5942 with $I > 2\sigma(I)$; refinement by full-matrix least-squares methods (based on F_o^2, SHELXL-97); anisotropic thermal parameters for all non-H atoms in the final cycles; the H atoms were refined on a riding model in their ideal geometric positions, except for H(11A), H(11B), H(15A), H(15B), H(19A), H(19B), H(23A), and H(23B), which were refined independently; $R1$ = 0.0592 [$I > 2\sigma(I)$], wR2(F_o^2) = 0.1635 (all data), absolute structure (Flack) parameter 0(2). The refinement of the correct stereoisomer is unambiguous due to the fixed absolute configuration at C(3), C(8), C(29), and C(34) of the (*R*,*R*)-TMCDA (Flack parameter not significant).

X-ray Structure Determination of 3b. (colorless needles from *n*-pentane/hexane, 0.30 × 0.30 × 0.20 mm^3): $C_{36}H_{80}Li_4N_4$, M = 596.8, triclinic, space group $P\bar{1}$ (No. 2), a = 13.427(5), b = 13.440(5), c = 24.950(9) Å, α = 101.217(9)°, β = 95.838(10)°, γ = 105.366(11)°, V = 4202(3) Å^3, Z = 4, D_c = 0.943 Mg m^{-3}, μ = 0.052 mm^{-1}. 32 682 reflections measured with 2θ in the range 1.61−24.00°, 13 210 unique reflections; 6671 with $I > 2\sigma(I)$; refinement by full-matrix least-squares methods (based on F_o^2, SHELXL-97); anisotropic thermal parameters for all non-H atoms in the final cycles; the H atoms were refined on a riding model in their ideal geometric positions, except for H(11A), H(11B), H(12A), H(12B), H(15)A, H(15B), H(16A), H(16B), H(19A), H(19B), H(23A), H(23B), H(24A), H(24B), H(47A), H(47B), H(48A), H(48B), H(51A), H(51B), H(55A), H(55B), H(56A), H(56B), H(59A), H(59B), H(60A), and H(60B), which were refined independently; R1 = 0.0769 [$I > 2\sigma(I)$], wR2(F_o^2) = 0.2336 (all data).

Theoretical Calculations. To verify experimental results, density functional theory (DFT) B3LYP calculations were performed with the program Gaussian 03.[14] The 6-31+G(d) and 6-31G basis sets were used; starting coordinates were obtained from the crystal structures or with Chem3DUltra 10.0. A summary of the Cartesian

(15) Optimization was performed at the B3LYP/6-31+G(d) level, and frequency analysis at B3LYP/6-31G. To obtain the ZPE on the higher level, the value of the zero-point correction was added to the SCF energy.

(16) Würthwein, E.-U.; Hoppe, D. *J. Org. Chem.* **2005**, *70*, 4443.

(17) For tetrameric methyllithium structures, see: (a) Lucken, E. A. C.; Weiss, E. *J. Organomet. Chem.* **1964**, *2*, 197. (b) Weiss, E.; Lambertsen., T.; Schubert, B.; Cockcroft, J. K.; Wiedenmann, A. *Chem. Ber.* **1990**, *123*, 79. (c) Weiss, E.; Lucken, E. A. C. *J. Organomet. Chem.* **1964**, *2*, 197. (d) Ogle, C. A.; Huckabee, B. K.; Johnson, H. C., IV; Sims, P. F.; Winslow, S. D.; Pinkerton, A. A. *Organometallics* **1193**, *12*, 1960. (e) Köster, H.; Thoennes, D.; Weiss, E. *J. Organomet. Chem.* **1978**, *160*, 1.

(18) (a) For methylation, see: Kizirian, J.-C.; Cabello, N.; Pinchard, L.; Caille, J.-C.; Alexakis, A. *Tetrahedron* **2005**, *61*, 8939. (b) For the resolution, see: Larrox, J. F.; Jacobsen, E. N. *J. Org. Chem.* **1994**, *59*, 1939.

coordinates and calculated energies of all minimum structures and transition states is provided in the Supporting Information.

Summary and Conclusion

In summary, the influence of *n*-butyllithium/ligand ratio on the degree of aggregation has been investigated. Two different types of adducts between *n*-BuLi and (*R*,*R*)-TMCDA were presented, the dimer [*n*-BuLi·(*R*,*R*)-TMCDA]$_2$ with 1 equiv of *n*-BuLi and the ladder structure [(*n*-BuLi)$_2$·(*R*,*R*)-TMCDA]$_2$ with 2 equiv of *n*-BuLi. Two isomers of the ladder structure could be isolated in the crystal, which differ in the arrangement of the three central Li−C−Li−C four-membered rings. These are the first homoaggregate of *n*-butyllithium with a ladder arrangement. Additionally, the ladder structure represents a transition from the hexameric (*n*-BuLi)$_6$ to the dimer [*n*-BuLi·(*R*,*R*)-TMCDA]$_2$. Based on these structures, theoretical studies on the reaction pathways of the deprotonation of benzene were performed, indicating possible mechanisms involving monomeric and dimeric structures.

Acknowledgment. We are grateful to the Deutsche Forschungsgemeinschaft and the Fonds der Chemischen Industrie for financial support and the award of a scholarship (to V.H.G.). Especially, we acknowledge Chemetall GmbH for providing us with special chemicals.

Supporting Information Available: DFT calculational output (Cartesian coordinates, calculated energies) and further crystallographic information (CIF). This material is available free of charge via the Internet at http://pubs.acs.org.

JA8017187